

Development of CMOS monolithic pixel sensors with in-pixel correlated double sampling and fast readout

Marco Battaglia, Jean-Marie Bussat, Devis Contarato, Peter Denes, Piero Giubilato, Lindsay E. Glesener

Abstract—This paper presents the design and results of detailed tests of a CMOS active pixel chip for charged particle detection with in-pixel charge storage for correlated double sampling and readout in rolling shutter mode at frequencies up to 25 MHz. This detector is developed in the framework of R&D for the Vertex Tracker for a future e^+e^- Linear Collider.

I. INTRODUCTION

THE Vertex Tracker for a future e^+e^- Linear Collider, such as the International Linear Collider (ILC) project, has requirements in terms of position resolution and material budget that largely surpass those of the detectors at LEP, SLC and LHC. The single point resolution needs to be $\leq 3 \mu\text{m}$ and the detector has to be read-out fast enough that the machine-induced background does not adversely affect the track pattern recognition and reconstruction accuracy. Detailed simulation of incoherent pair production in the strong field of the colliding beams, the dominant background source, predicts a hit density of order of 5 hits bunch crossing $^{-1} \text{cm}^{-2}$ on the innermost detector layer, located at a radius of 1.5 cm from the interaction point, for 250 GeV beams and a solenoidal field of 4 T. The requirement of a hit occupancy $\leq 0.1 \%$, needed to ensure clean standalone pattern recognition in the Vertex Tracker, corresponds to a maximum of 80 bunch crossings which can be integrated by the detector in a readout cycle, i.e. a readout frequency of 25 MHz for a detector with 512 pixel long columns. Finally, power dissipation must be kept small enough, so that cooling can be achieved by airflow, without requiring active cooling systems that contribute significantly to the material budget of the vertex detectors installed in the LHC experiments. Tests performed on a carbon composite

prototype ladder, equipped with $50 \mu\text{m}$ -thin CMOS pixel sensors, have shown that an airflow of 2 m s^{-1} can remove $\simeq 80 \text{ mW cm}^{-2}$. Assuming a pixel column made of 512 pixels, this corresponds to a maximum allowable power dissipation of $\simeq 0.5 \text{ mW column}^{-1}$.

An attractive sensor architecture for the Linear Collider Vertex Tracker sensor is a pixel of $\simeq 20 \times 20 \mu\text{m}^2$ readout at 25–50 MHz during the long ILC bunch train. Signals are digitised at the end of the column with enough accuracy to allow charge interpolation to optimise the spatial resolution. Digitising at the required speed and within the maximum tolerable power dissipation poses major design challenge. The study of data collected with a CMOS pixel test chip, with $10 \times 10 \mu\text{m}^2$, $20 \times 20 \mu\text{m}^2$ and $40 \times 40 \mu\text{m}^2$ pixels [1], shows that a 5-bit ADC accuracy is sufficient, provided that pixel pedestal levels are subtracted before digitisation. This requires performing pedestal subtraction either in pixel or at the end of the column.

II. LDRD-2: A PIXEL CHIP WITH IN-PIXEL CDS

We have designed a CMOS monolithic pixel chip with in-pixel correlated double sampling (CDS) and tested it for readout speeds up to 25 MHz. The chip consists of a matrix of 96×96 pixels arrayed on a $20 \mu\text{m}$ pitch. Each pixel has two $5 \times 5 \mu\text{m}^2$ polysilicon-insulator-polysilicon (PIP) capacitors, corresponding to a capacitance of $\simeq 20 \text{ fF}$. These capacitors are used for the storage of the pixel reset and signal levels. The net pixel signal is obtained by subtracting the reset from the signal level. In the current CDS implementation, this subtraction is performed off-chip, allowing for a detailed performance study. Pixels are readout in rolling shutter mode, which ensures a constant integration time across the pixel matrix. The pixel array is divided in two 48×96 pixel sections, which are readout in parallel. Different pixel designs, including diode sizes of $3 \mu\text{m}$ and $5 \mu\text{m}$, have been implemented. One half of the pixel matrix implements charge-collection diodes surrounded by a guard-ring in order to study the effect of a guard-ring after irradiation.

The detector has been fabricated in an AMS $0.35 \mu\text{m}$ 4-metal, 2-poly CMOS-OPTO process, which provides an epitaxial layer with a nominal thickness of $14 \mu\text{m}$.

The readout sequence is as follows. On a reset signal on the pixel i , the pixel reset level is stored and the charge is integrated on the diode, while the reset level is stored for the pixel $i + 1$. After the integration time which corresponds to the scan of a section, i.e. N_p/f , where N_p is the number of

Manuscript received May 30, 2008. We thanks the staff of the LBNL ALS and 88" cyclotron and of the FNAL MTBF for their assistance during data taking and the excellent performance of the accelerators. This work was supported by the Director, Office of Science, of the U.S. Department of Energy under Contract No.DE-AC02-05CH11231.

M. Battaglia is with the Department of Physics, University of California and the Lawrence Berkeley National Laboratory, Berkeley, CA 94720, USA (telephone: 510-486-7029, e-mail: mbattaglia@lbl.gov).

J.M. Bussat was with the Lawrence Berkeley National Laboratory, Berkeley, CA 94720, USA, now is with Stanford University, CA 94305, USA

D. Contarato is with the Lawrence Berkeley National Laboratory, Berkeley, CA 94720, USA

P. Denes is with the Lawrence Berkeley National Laboratory, Berkeley, CA 94720, USA

P. Giubilato is with the Istituto Nazionale Fisica Nucleare, Sezione di Padova, Italy and a visitor at the Lawrence Berkeley National Laboratory, Berkeley, CA 94720, USA

L.E. Glesener is with the Department of Physics, University of California and the Lawrence Berkeley National Laboratory, Berkeley, CA 94720, USA

pixels in a readout section and f the readout frequency, the signal level is stored, the pixel is reset and the cycle restarted. The reset and signal levels are readout serially. The highest frequency tested is 25 MHz, corresponding to an integration time of 184 μ s. In order to minimise the power dissipation of the pixel cell, the source follower is switched on only in the short time elapsed between the write signal level of one event and the write reset level of the next event.

The detector is readout through a custom FPGA-driven acquisition board. The board has four 14 bit, 40 MSample/s TI ADS5421 ADCs which read the chip outputs, while an array of digital buffers drives all the required clocks and synchronisation signals. For each of the 48×96 pixel halves, the signal and reset levels stored in the in-pixel capacitors are sent to two different analog outputs which are subsequently digitised by two different ADCs on the readout board. The FPGA has been programmed to generate the clock pattern and collect the sampled data from the ADCs. A 32 bit wide bus connects the FPGA to a NI-6533 digital acquisition board installed on the PCI bus of the control PC. Data are processed on-line by a LabView-based program, which performs the subtraction of the reset level from the pixel level and computes the pixel noise and residual pedestal.

III. PIXEL RESPONSE TESTS

The detector has been tested in the lab using a 2.2 mCi ^{55}Fe collimated source. The detector performance has been studied as a function of the readout frequency, from 1.25 MHz up to 25 MHz. First the pixel noise has been measured for operation at room temperature. No significant degradation of the noise of the pixel matrix is observed up to the highest frequency. The measured noise is due, in part, to the readout electronics noise, which has been estimated to be $\simeq 20$ ENC. The pixel noise has been studied as a function of the operating temperature (from $+20$ $^{\circ}\text{C}$ to -20 $^{\circ}\text{C}$). We measure (42 ± 4) ENC, (54 ± 7) ENC and (54 ± 6) ENC at $+20$ $^{\circ}\text{C}$ and (37 ± 6) ENC, (43 ± 5) ENC and (46 ± 5) ENC at -20 $^{\circ}\text{C}$, at readout frequencies of 1.25 MHz, 6.25 MHz and 25 MHz, respectively, where the quoted uncertainties represent the spread of the noise measured on the pixels of a sector.

The pixel calibration has been obtained using the 5.9 keV X-rays from a ^{55}Fe source for various readout frequencies. Charge generated by X-rays which convert in the shallow depletion region near the pixel diode is fully collected, resulting in a pulse height peak corresponding to the full X-ray energy, which generates on average 1640 electrons in the Si sensitive volume. We select pixel clusters consisting of either a single pixel with a pulse height in excess of seven times the pixel noise or a pixel fulfilling the same requirement plus an adjacent pixel with pulse height in excess of three times the pixel noise. The resulting pulse height spectra are shown in Figure 1, for different readout frequencies.

The response to high momentum particles has been studied in beam tests. We used both the 1.35 GeV electron beam from the LBNL Advanced Light Source (ALS) booster and the 120 GeV secondary proton beam at the Meson Test Beam Facility (MTBF) at Fermilab, as part of the T966

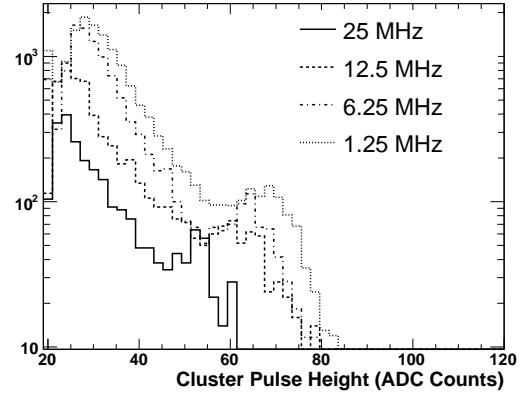


Fig. 1. Response of the LDRD-2 chip to 5.9 keV X-rays from ^{55}Fe for readout frequencies of 1.25 MHz (dotted), 6.25 MHz (dash dotted), 12.5 MHz (dashed) and 25 MHz (continuous).

beam test experiment [2]. Data are converted into the `lcio` format [3], which is the persistency format adopted by the ILC studies. The data analysis is performed offline by a dedicated set of processors developed in the Marlin C++ framework [4]. Events are first scanned for noisy pixels. The

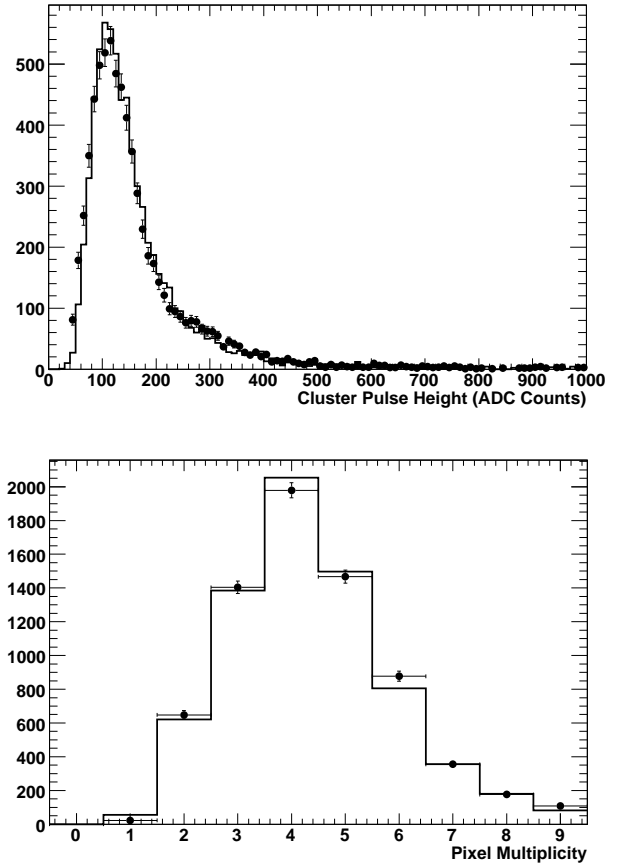


Fig. 2. Response of the LDRD-2 pixel chip to 1.35 GeV e^- : Data (points with error bars) are compared to predictions from our simulation based on GEANT-4 and a dedicated sensor simulation in Marlin (line) for the cluster pulse height (above) and pixel multiplicity in the cluster (below).

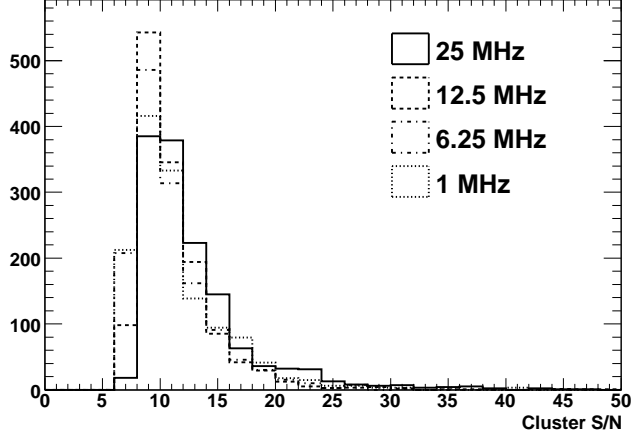


Fig. 3. Response of the LDRD-2 chip for various readout frequencies: cluster signal-to-noise distributions for 1.35 GeV e^- s for readout 1 MHz (dotted), 6.25 MHz (dash dotted), 12.5 MHz (dashed) and 25 MHz (continuous).

noise and pedestal values computed on-line are updated, using the algorithm in [5], in order to follow possible variations in the course of a data taking run.

A cluster search is performed next. Each event is scanned for pixels with pulse height values over a signal-to-noise (S/N) threshold of 5, these are designated as cluster ‘seeds’. Seeds are then sorted according to their pulse heights and the surrounding, neighbouring pixels are tested for addition to the cluster. The neighbour search is performed on a 7×7 matrix

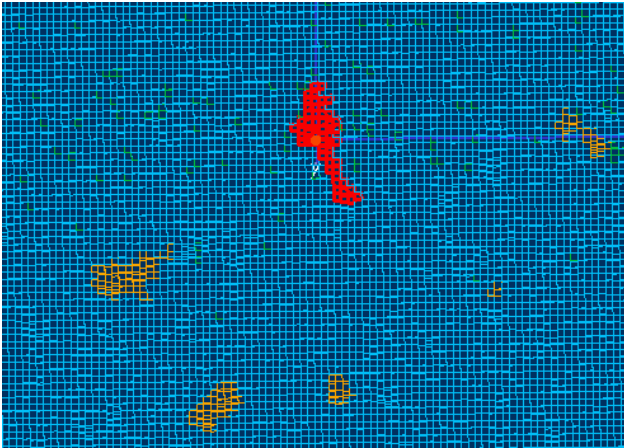


Fig. 4. LDRD-2 response to low momentum electrons. This event display shows clusters produced by low momentum electrons produced by the interaction of 1.35 GeV electrons on an Al scraper. Clusters are evidently broad and asymmetric.

surrounding the pixel seed and the neighbour threshold is set at 2.5, in units of the pixel noise. Clusters are not allowed to overlap, i.e. pixels already associated to one cluster are not considered for populating another cluster around a different seed. Finally, we require that clusters are not discontinuous, i.e. pixels associated to a cluster cannot be separated by any pixel below the neighbour threshold. The expected pixel response is simulated with a dedicated digitisation processor in Marlin [6]. The charge collection process is described

starting from ionisation points generated along the particle trajectory using Geant 4 [7], by modelling the diffusion of charge carriers, originating in the epitaxial layer, to the collection diode. Simulated data are then processed through the cluster reconstruction stage, using the same processor as beam test data. A comparison of the real and simulated cluster pulse height and pixel multiplicity obtained, after tuning the charge carrier diffusion length in simulation to provide the best fit to the pixel multiplicity distribution, is shown in Figure 2. Finally, the response to low momentum electrons has been studied. The response of the detector to low energy electrons is important since particles from pair background have energies typically below 100 MeV. Data has been collected at the ALS with an Al beam scraper placed a few meters upstream of the LDRD-2 detector. A large fraction of the registered hits are due to low energy electrons, originating from the interaction of the primary beam with the Al scraper, or to tertiaries, from photon conversions. These hits are characterised by large, asymmetric clusters (see Figure 4) with average multiplicity exceeding 1.5 times that of clusters from high energy electrons. This suggests that low-energy background hits could be identified and rejected, based on the observed cluster shape.

The response to high energy hadrons has been studied with 120 GeV protons at MTBF. The most probable cluster pulse height has been measured to be $(1112 \pm 17) e^-$ s for $5 \mu\text{m}$ and $(830 \pm 13) e^-$ s for $3 \mu\text{m}$ collecting diodes as shown in Figure 5. The most probable pixel multiplicity scales from 2.7 to 4.3, respectively. An average signal-to-noise ratio of 12 to 13 has been measured for 1 MHz and 25 MHz readout, respectively (see Figure 3). The detector was operated at $+20^\circ\text{C}$ and the signal-to-noise performance is limited in part by the noise of the read-out board, as discussed above.

IV. RADIATION HARDNESS TESTS

At an e^+e^- linear collider there are two main sources of radiation, which need to be considered to assess the radiation tolerance of the sensor. The first is due to low energy neutrons produced by giant resonance excitations in the beam dump and in the interaction of low energy pair background on the forward masks. The neutrons at the location of the Vertex Tracker has been estimated to generate a fluence $\simeq 6 \times 10^{10} \text{ n cm}^{-2} \text{ year}^{-1}$. The second radiation source is due to low momentum pairs produced in the electromagnetic interaction of the colliding beams corresponding to a dose of $\simeq 50 \text{ kRad/year}$ on the Vertex Tracker.

The effect of ionising radiation has been assessed by exposing the chip to 200 keV electrons at the 200 CX electron microscope of the National Center for Electron Microscopy at LBNL. Electrons of 200 keV are below the displacement damage threshold for Si. The sensor has been irradiated with a flux of $\simeq 2300 e^- \text{ s}^{-1} \mu\text{m}^{-2}$, in multiple steps. In between consecutive irradiation steps, 100 events are acquired without beam and the pixel pedestals and noise computed, in order to monitor the evolution of the pixel leakage current with dose. Figure 6 shows the pixel pedestal levels, which measure the leakage current, as a function of the integrated dose. All tests have been performed at room temperature. Results show that

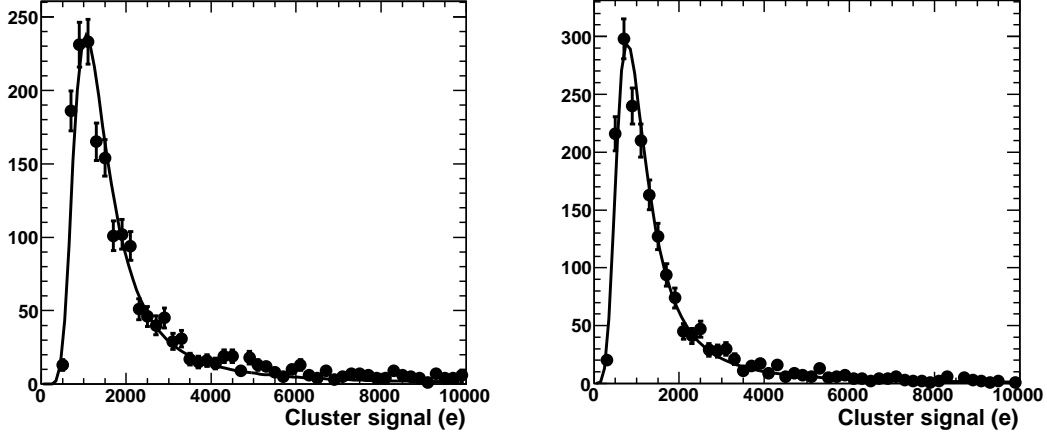


Fig. 5. Response of the LDRD-2 pixel chip to 120 GeV protons: Cluster pulse height distributions obtained for pixels with 5 μm (left) and 3 μm (right) diode. The continuous lines show the interpolated Landau functions.

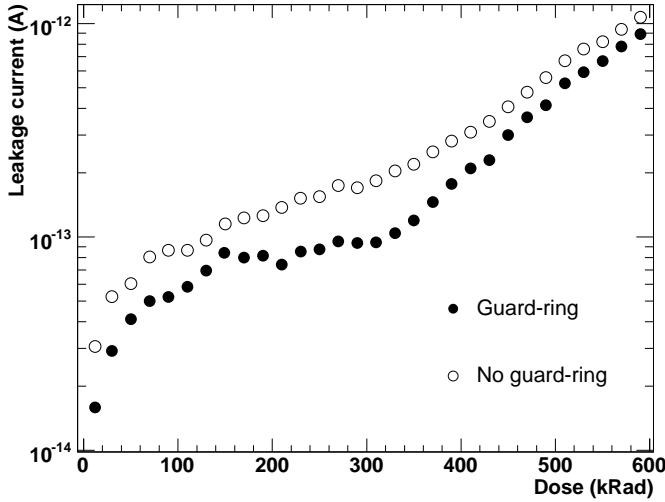


Fig. 6. Results of the LDRD-2 sensor irradiation with 200 keV electrons. Sensor leakage current as a function dose for pixel cells designed with (filled dots) and without (open dots) guard ring around the charge-collecting diode.

the pixel functions properly up to several hundreds kRads, i.e. doses comparable to five or more year of operation at a linear collider, with leakage currents below 1 pA which is an acceptable level and can be further controlled by cooling the device during operation. The effect of a guard-ring around the charge-collecting diode is also apparent.

The effect of non-ionising radiation has been studied exposing the LDRD-2 detector chip to neutrons produced from 20 MeV deuteron breakup on a thin target at the LBNL 88-inch cyclotron [8]. The detector chip was located 8 cm downstream from the target and activation foils were placed just behind it to monitor the fluence. Deuteron breakup produces neutrons on a continuum spectrum from < 1 MeV up to ~ 14 MeV. A beam current of 800 nA was used, corresponding to an estimated flux at the chip position of $\simeq 4 \times 10^8 \text{ n cm}^{-2} \text{ s}^{-1}$. We compared the pixel noise before and after irradiating the chip with a

total fluence of $1.2 \times 10^{13} \text{ n cm}^{-2}$. As the observed increase in noise of $(7 \pm 8) e^-$ is not significant, the test shows that the chip can withstand neutrons fluxes significantly above those foreseen at the interaction region of an e^+e^- linear collider.

V. CONCLUSIONS AND OUTLOOK

The LDRD-2 pixel cell has small pitch and in-pixel charge storage for correlated double sampling. This offers a viable architecture for a pixel sensor with analog readout able to match the timing requirements of the Vertex Tracker at a linear collider such as the ILC. The chips has been characterised using ^{55}Fe and particle beams. The chip performance is found to be stable up to the highest tested readout frequency of 25 MHz, corresponding to an integration time of 184 μs . The radiation tolerance of the pixel cell has been tested with low-energy electrons and neutrons. The pixel withstands radiation fluxes in excess to those expected after several years of operation in the Vertex Tracker of an e^+e^- linear collider. The pixel cell is the basis of a third-generation chip, which further addresses the requirements of the ILC, or other future e^+e^- linear colliders. The LDRD-3 chip consists of a matrix of 96×96 pixels on a 20 μm pitch, with the same pixel cell as the LDRD-2. In addition, the chip features a column parallel readout at frequency up to 50 MHz and the digitisation is performed on-chip, at the end of each column, by a row of successive approximation, fully differential ADCs featuring low power dissipation. Each ADC has a size of 20 $\mu\text{m} \times 1 \text{ mm}$, which matches the pixel pitch. The digitisation of the 96 rows is performed in 1.9 μs .

REFERENCES

- [1] M. Battaglia *et al.*, In the *Proceedings of International Symposium on Detector Development for Particle, Astroparticle and Synchrotron Radiation Experiments (SNIC 2006)*, Menlo Park, California, 3-6 Apr 2006, pp 0108.
- [2] M. Battaglia *et al.*, Nucl. Instrum. Meth. A **593** (2008) 292 [arXiv:0805.1504 [physics.ins-det]].
- [3] F. Gaede, T. Behnke, N. Graf and T. Johnson, in the *Proc. of 2003 Conf. for Computing in High-Energy and Nuclear Physics (CHEP 03)*, La Jolla, California, 24-28 Mar 2003, pp TUKT001, [arXiv:physics/0306114].

- [4] F. Gaede, Nucl. Instrum. Meth. A **559** (2006) 177.
- [5] V. Chabaud *et al.*, Nucl. Instrum. Meth. A **292** (1990) 75.
- [6] M. Battaglia, Nucl. Instrum. Meth. A **572** (2007) 274.
- [7] S. Agostinelli *et al.*, Nucl. Instrum. Meth. A **506** (2003), 250.
- [8] M.A. McMahan, Nucl. Instrum. Meth. B **261** (2007), 974.